
Flip Initial Features: Generalization of Neural Networks Under Sparse Features for Semi-supervised Node Classification

Yoonhyuk Choi¹

Jiho Choi¹

Taewook Ko¹

Chong-Kwon Kim²

¹Computer Science Dept., Seoul National University, Seoul, South Korea

²Energy AI Dept., Korea Institute of Energy Technology, Naji, South Korea

Abstract

Graph neural networks (GNNs) have been widely used under semi-supervised settings. Prior studies have mainly focused on finding appropriate graph filters (e.g., aggregation schemes) to generalize well for both homophilic and heterophilic graphs. Even though these approaches are essential and effective, they still suffer from the sparsity in initial node features inherent in the bag-of-words representation. Common in semi-supervised learning where the training samples often fail to cover the entire dimensions of graph filters (hyperplanes), this can precipitate over-fitting of specific dimensions in the first projection matrix. To deal with this problem, we suggest a simple and novel data augmentation strategy; create additional space by flipping the initial features and hyperplane simultaneously. Training in both the original and the flip space can provide precise updates of learnable parameters and secure robustness for unseen features during inference. To the best of our knowledge, this is the first attempt that effectively moderates the overfitting problem in GNN. Extensive experiments on real-world datasets demonstrate that the proposed technique improves the node classification accuracy by up to 40.2 %.

1 INTRODUCTION

With the flux of graphical data, graph neural networks (GNNs) accomplished prominent improvement in various fields. By integrating node features and network structures concurrently, they have shown the powerful ability for node and graph classification tasks [Defferrard et al., 2016, Kipf and Welling, 2016, Hamilton et al., 2017, Velickovic et al., 2017]. Message passing, which aggregates features from neighbor-

ing nodes recursively, is a key mechanism of GNNs [Gilmer et al., 2017].

Recently, many studies have focused on the amelioration of an aggregation scheme to deal with heterogeneous (disassortative) edges. Generally, GNNs fully enjoy the advantage of message passing in homophilic graphs [McPherson et al., 2001]. But in heterogeneous graphs, they struggle to find homophilic neighbors to secure robustness. Several algorithms assign different weights to edges before aggregation [Velickovic et al., 2017, Yang et al., 2019, Bo et al., 2021, Kim and Oh, 2022] or even eliminate disassortative edges [Ying et al., 2019, Luo et al., 2021]. Others further utilize distant nodes with high similarity [Pei et al., 2020, Jin et al., 2021] or adopt node-specific propagation using trainable boundaries [Xiao et al., 2021]. We fully understand that the proper selection of aggregation schemes is essential. Nonetheless, we raise another question: *are there other aspects beyond aggregation schemes?*

Contrary to previous approaches, we concentrate on the training mechanism of weight matrices (hyperplanes). Our quest originates from an observation that if initial features contain a few non-zero elements (e.g., bag-of-words), insufficiency in training samples (semi-supervised settings) causes overfitting of specific dimensions in the first layer parameters (please refer to Appendix A for details). Both initial features well classify nodes in this two dimension example, but if the dimensionality is large, the first hyperplane might be biased in certain dimensions. We emphasize that this can harm the quality of predicting test nodes that contain untrained dimensional features.

To better optimize the feature transformation matrix, we focus on the perturbation of the initial features. Our initial choice was a data augmentation mechanism like dimensional image shifting used in computer vision [Shijie et al., 2017]. However, we concluded that shifting is not applicable to GNNs with bag-of-words features where a bit position itself has a specific meaning; positional shifting disarranges the semantic information. Also, compared to

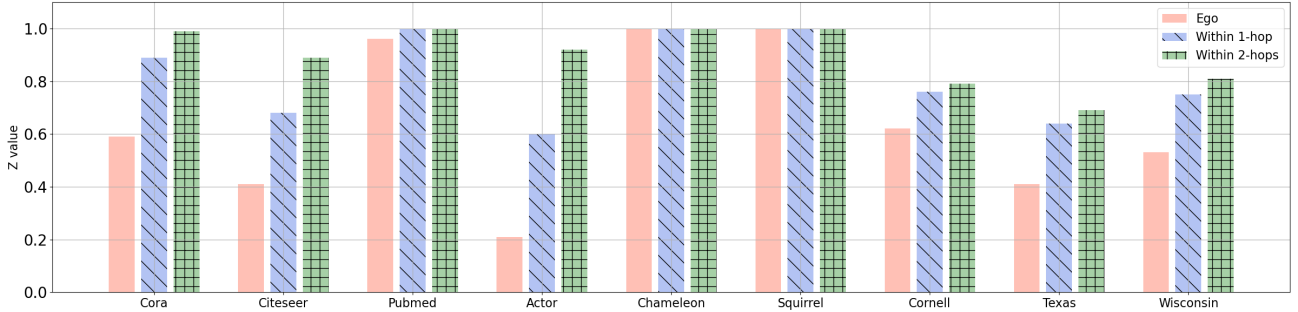


Figure 1: Initial feature distribution of each graph dataset. The definition of value Z is described in Equation 1

the convolutional neural network which ensures local invariance [Zhang et al., 2017], GNNs employ multi-layer perceptron (MLP) which is not translation invariant. We also considered adding a noise [Zhu et al., 2021] to inputs. But, this requires an additional decoding process with a precise selection of hyperparameters and also implicates a normalization problem [Cai et al., 2021].

We devise a solution that flips the initial features and parameters simultaneously. The proposed flipping scheme is inspired by previous techniques of shifting parameters [Kim et al., 2019] and rotation of neural networks [Lin et al., 2020] which can preserve the volume of gradients and initial features. We also focus on a dual path network [Chen et al., 2017b] that a slight change of parameter can ensure our model operates in the original and flipped spaces concurrently. Our method solves the zero gradient problem caused by input data and also facilitates accurate semantic learning of each dimension [Liu et al., 2022]. The flipping mechanism is orthogonal to GNNs and we apply the flipping mechanism to three representative methods (MLP, GCN, and GAT). We compare the performances of the three variants with state-of-the-art baselines on nine real-world datasets. We observe that the average gain of the three flipping methods, Flip-MLP, Flip-GCN, and Flip-GAT over their originals are 16.5 %, 24.2 %, and 17.8 %, respectively. The contributions can be summarized as follows:

- We show that GNNs are quite sensitive to initial features and their performance can be largely improved if zero elements are eliminated.
- To solve the problem, we propose a flipping mechanism that concurrently transposes initial features and hyperplane. Unlike previous methods that focus on aggregation schemes, our method scrutinizes the back-propagation and subsidizes precise component-wise guiding of the first hyperplane.
- The proposed flipping mechanism is orthogonal to GNNs. Applying flipping to MLP, GCN, and GAT. we develop three flipping variants. We conduct extensive experiments using real-world benchmark graphs. The flipping variants surpass all state-of-the-art baselines.

2 PRELIMINARIES

This section starts with the feature distribution of benchmark datasets. Then, we define the widely used notations in the Graph Neural Network (GNN) that will be used throughout this paper. Finally, we describe the basic mechanisms of several GNN algorithms.

2.1 EMPIRICAL ANALYSIS

We conduct an empirical study to show the ratio of non-zero elements of each dataset. Firstly, let us define z as below:

$$Z = \frac{\# \text{ of non-zero feature dimension in training nodes}}{\# \text{ of entire feature dimension}} \quad (1)$$

The numerator contains the elements of all training nodes whose values are non-zero. In Figure 1, we describe the Z of each graph by varying the range of neighbors from ego to 2-hop adjacent nodes. We can see that the value of Z increases in proportion to the range since more features are available during the training phase. We also observe that values Z of datasets are quite different. As we will explain later, the experimental results show that the lower this value of a network is, the greater the performance improvement that flipping achieves. We insist that the z-value of ego is dominant for gradient updates because of the degree-based normalization (please see Section 4.4 for details).

2.2 NOTATIONS

Let $\mathcal{G} = (\mathcal{V}, \mathcal{E})$ be an undirected graph that contains $|\mathcal{V}| = n$ nodes and $|\mathcal{E}| = m$ edges. Let $A \in \{0, 1\}^{n \times n}$ be an adjacency matrix determined by the connectivity of a graph. In many cases, it is available to utilize a feature matrix $X \in \mathbb{R}^{n \times F}$ that comprise the properties of the entire nodes, where F is the input dimension of initial features. Each node has its label that is represented as $Y \in \mathbb{R}^{n \times C}$. Here, C is the number of labels (classes). We separate the first layer weight matrix of GNN into two parts W_o and W_f , where the lower script o and f denote an original and flipped space, respectively. A symbol ∇ represents a partial derivative.

Our goal is to solve a node classification task under semi-supervised settings, where the labeled nodes $\mathcal{V}_L \subset \mathcal{V}$ are partially available as a training set. GNNs focus on how to better utilize the given information for the prediction of unlabeled nodes $\mathcal{V}_U = \mathcal{V} - \mathcal{V}_L$.

2.3 GRAPH NEURAL NETWORK

We focus on spatial GNNs which can reduce the computational cost of Laplacian decomposition. Their basic form is as below:

$$\begin{aligned} H^{(l+1)} &= \sigma(\bar{H}^{(l+1)}), \quad \bar{H}^{(l+1)} = \hat{A}H^{(l)}W^{(l)} \quad (l \geq 1) \\ \hat{Y} &= \text{softmax}(\bar{H}^{(L)}). \end{aligned} \quad (2)$$

\hat{A} stands for a matrix that is used for message passing. $H^{(1)} = X$ is an initial feature of nodes and $H^{(l)}$ is their representations at the l -th hidden layer. $\bar{H}^{(l)}$ is a vector at the l -th layer before activation σ (e.g., ReLU). Applying softmax on the output $\bar{H}^{(L)}$, GNNs obtain the final prediction. $W^{(l)}$ is the trainable weight matrices at the l -th layer shared across all nodes. They are updated through negative log-likelihood loss \mathcal{L}_{nll} between the predicted \hat{Y} and true labels Y as below:

$$\mathcal{L}_{GNN} = \mathcal{L}_{nll}(Y, \hat{Y}). \quad (3)$$

GNNs [Velickovic et al., 2017, Klicpera et al., 2018, Chen et al., 2020a, Bo et al., 2021] have their unique aggregation schemes (finding appropriate \hat{A}). For example, GCN [Kipf and Welling, 2016] takes the normalized Laplacian and GAT [Velickovic et al., 2017] constructs an aggregation matrix by computing attention score between two nodes. Now, we introduce the motivation and the necessity of our algorithm in the following section.

3 METHODOLOGY

3.1 MOTIVATION

We first explain the limitation of the generic GNN mechanism. It is undeniable that appropriate aggregation schemes are essential for securing the proper performance of GNNs. However, as explained below, an aggregation scheme alone cannot avoid the improper learning problem rooted in the sparseness of the initial features. More specifically, we first scrutinize the backpropagation of GNNs:

$$\nabla_{W^{(l)}} J = (\hat{A}H^{(l)})^T \nabla_{\bar{H}^{(l+1)}} J, \quad l = 1, \dots, L. \quad (4)$$

Here, $J = \mathcal{L}_{GNN}$ represents a full-batch gradient of loss defined in Equation 3. As described in the above equation, the sparseness of \hat{A} can obstruct the gradient flow between dissimilar nodes. Unfortunately, there arises a problem when

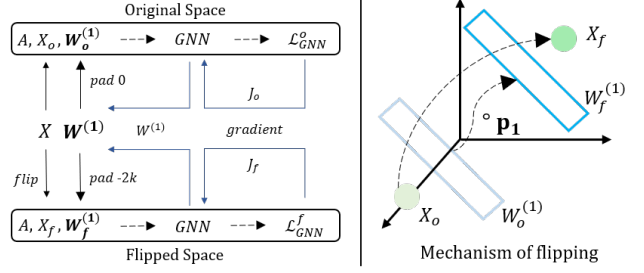


Figure 2: The overall architecture of Flip-GNN (left) and mechanism of flipping (right). The hyperplane $W^{(1)}$ is updated iteratively on both spaces

updating the parameters of initial layer $W^{(1)}$ as:

$$\begin{aligned} \nabla_{W^{(1)}} J &= (\hat{A}H^{(1)})^T \nabla_{\bar{H}^{(2)}} J \\ &= (\hat{A}X)^T \nabla_{\bar{H}^{(2)}} J. \end{aligned} \quad (5)$$

The above equation implies that the gradients become zero for certain dimensions with zero inputs. Thus, aggregation itself cannot handle the precise update of the first hyperplane $W^{(1)}$, necessitating a sparseness removal mechanism for the initial features X . To enable $W^{(1)}$ to learn the precise meaning of each dimension, we suggest flipping which is simple but is effective for semi-supervised learning.

The inadequate gradient update problem described before can be more conspicuous in semi-supervised learning. A simple remedy to the problem is shifting which is popularly used in computer vision. To remove zero signals, shifting adds a vector X_s , which consists of elements of small values, to the input features X as below:

$$X = X + X_s. \quad (6)$$

However, shifting may not be applicable to GNNs because MLP is not shift-invariant and can deteriorate robustness [Singla et al., 2021]. Further, it changes the magnitude of an input which is critical to the normalization of neural networks. Rotation can be a solution, but there exists a probability that the elements have negative values. For a more rigorous investigation of shifting, we devise a simple method that combines shifting with GCN and describes their performance in Appendix B. Now, we detail the training mechanism of GCN in the flipped space accompanied by parameter adjustment.

3.2 FLIPPED GRAPH NEURAL NETWORKS

We develop a scheme that flips both feature vectors and the hyperplane concurrently. If an original feature all of whose elements belong to $[0, 1]$, its symmetric transposition through $p = (0.5, \dots, 0.5)$ also resides in this range. (See the hypercube in the upper, left-most graphs in Figure 2 where a red point $(1,0,0)$ transpositions to $(0,1,1)$) This

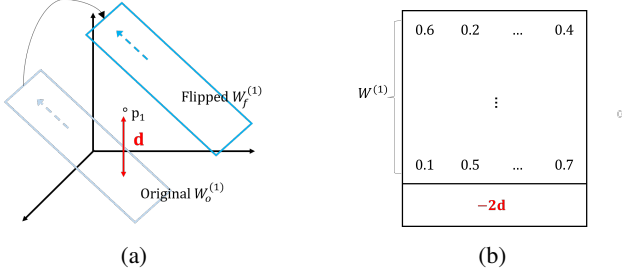


Figure 3: (a) Distance d from $W^{(1)}$ to p_1 . (b) $W_o^{(1)}$ is retrieved through zero-padding to the last dimension of $W^{(1)}$, while $W_f^{(1)}$ pads $-2d$

transposition is also applicable to the hyperplane $W^{(1)}$. In Figure 2, the upper and lower panels describe the original and flipped spaces, respectively. Even though the proposed flipping scheme is orthogonal to GNN techniques, We take GCN as a convolution layer as defined in Eq. 2. We apply flipping to MLP and GAT and obtain Flip-MLP and Flip-GAT as demonstrated in Appendix D.

Original space. Back to Figure 2, the upper panel is the same as plane GCN [Kipf and Welling, 2016]. The original feature (X_o) inherits X and fills the values of the last row as 0. Similarly, $W^{(1)}$ is zero-padded as below (this will be explained later):

$$X_o[F:] = 0, \quad W_o^{(1)} = \begin{pmatrix} W^{(1)} \\ 0 \end{pmatrix}. \quad (7)$$

Now, we can compute the loss $J_o = \mathcal{L}_{GNN}(Y, \hat{Y}_o)$ through Eq. 2 and 3, then update the parameter W .

Before introducing the flipped space, we first define some symbols. $p_1 = (0.5, \dots, 0.5, 0) \in \mathcal{R}^{F+1}$ and $p_2 = (0, \dots, 0) \in \mathcal{R}^{F'}$ are two datum points that are used for flipping. The last dimension of p_1 is zero-padded to be in line with $X \in \mathcal{R}^{n \times (F+1)}$ and $W^{(1)} \in \mathcal{R}^{(F+1) \times F'}$ where F and F' are the dimensions of the initial feature and the vector after the first projection, respectively.

Flipped space. The flipped features X_f are obtained by transposing the original features X through p_1 as below:

$$X_f = 2p_1 - X_o. \quad (8)$$

We should also flip the first hyperplane $W^{(1)}$ as described in Figure 3a. Firstly, we need to calculate a distance vector $d \in \mathcal{R}^{F'}$ between the original hyperplane $W_o^{(1)}$ and p_1 as follows:

$$d = \sum_{j=0}^F (p_1 \otimes W_o^{(1)})[:, j], \quad (9)$$

$$W_f^{(1)} = \begin{pmatrix} W^{(1)} \\ -2d \end{pmatrix}$$

, where \otimes is an element-wise product. Referring to Figure 3b, $W_f^{(1)}$ is retrieved by padding $-2d$ to the last element.

Algorithm 1 The overall mechanism of Flip-GCN

Require: Adjacency matrix A , node features X , parameters θ_G , epoch K , best valid and test acc. $\gamma' = \delta' = 0$, learning rate η

Ensure: Node classification accuracy δ'

- 1: **for** number of training epoch K **do**
 - 2: # GCN in original space
 - 3: **for** training samples **do**
 - 4: Given X , retrieve the \mathcal{L}_{GNN} (Eq. 3)
 - 5: Update $\theta_G^{k+1} = \theta_G^k - \eta \frac{\partial \mathcal{L}_{GNN}}{\partial \theta_G^k}$
 - 6: **end for**
 - 7: Compute the validation γ and test score δ
 - 8: **if** $\gamma > \gamma'$ **then**
 - 9: $\gamma' = \gamma, \delta' = \delta$
 - 10: # GCN in flipped space
 - 11: **for** training samples **do**
 - 12: Flip initial features using Eq. 8
 - 13: Flip the first hyperplane through Eq. 9
 - 14: Compute \mathcal{L}_{GNN}^f in Eq. 11
 - 15: Update $\theta_G^{k+2} = \theta_G^{k+1} - \eta \frac{\partial \mathcal{L}_{GNN}^f}{\partial \theta_G^{k+1}}$
 - 16: **end for**
 - 17: Compute the validation γ and test score δ
 - 18: **if** $\gamma > \gamma'$ **then**
 - 19: $\gamma' = \gamma, \delta' = \delta$
 - 20: **end for**
-

We can assure the p_2 (origin) symmetry after the first convolution as $XW_o^{(1)} = -X_fW_f^{(1)}$. In the flipped space, we should also flip the sign of the output $\sigma(\hat{A}X_fW_f^{(1)})$ before the next convolution layer as follows:

$$H_f^{(2)} = -\sigma(\hat{A}X_fW_f^{(1)}), \quad (l=1)$$

$$H_f^{(l+1)} = \sigma(\bar{H}_f^{(l+1)}), \quad \bar{H}_f^{(l+1)} = \hat{A}H_f^{(l)}W^{(l)}, \quad (l \geq 2) \quad (10)$$

The loss \mathcal{L}_{GNN}^f can be computed using the final representation $\bar{H}_f^{(L)}$ as below:

$$\mathcal{L}_{GNN}^f = \mathcal{L}_{nll}(Y, \hat{Y}_f), \quad \hat{Y}_f = \text{softmax}(\bar{H}_f^{(L)}). \quad (11)$$

Based on Eq. 11, $W^{(1)}$ can be trained in the flipped space. We describe the mechanism of our method in Algorithm 1.

3.3 OPTIMIZATION STRATEGY

We define two loss functions in Equation 3 and 11. For gradient analyses, it is worth noting the following equation:

$$H^{(2)} = \sigma(\hat{A}X_oW_o^{(1)}) = H_f^{(2)} = -\sigma(\hat{A}X_fW_f^{(1)}) \quad (12)$$

, which implies that the outputs (or gradients) of two different spaces are equivalent after two layers as below:

$$\nabla_{W_o^{(l)}} J_o = \nabla_{W_f^{(l)}} J_f, \quad (l \geq 2). \quad (13)$$

Table 1: Statistical details of nine benchmark graph datasets

Datasets	Cora	Citeseer	Pubmed	Actor	Chameleon	Squirrel	Cornell	Texas	Wisconsin
# Nodes	2,708	3,327	19,717	7,600	2,277	5,201	183	183	251
# Edges	10,558	9,104	88,648	25,944	33,824	211,872	295	309	499
# Features	1,433	3,703	500	931	2,325	2,089	1,703	1,703	1,703
# Classes	7	6	3	5	5	5	5	5	5
# Training Nodes	140	120	60	100	100	100	25	25	25
# Validation Nodes	1,568	2,207	18,657	3,750	1,088	2,550	79	79	113
# Test Nodes	1,000	1,000	1,000	3,750	1,089	2,551	79	79	113

Similar to J_o , $J_f = \mathcal{L}_{GNN}^f$ is a full-batch gradient in the flipped space (Eq. 11). Even though Sigmoid or Tanh guarantees a perfect symmetry $J_o = J_f$, we employ ReLU for better performance. Now, referring to Eq. 5, we define the gradients of the first hyperplane $W^{(1)}$ on both spaces as,

In the original space, update $W_o^{(1)}$:

$$\nabla_{W_o^{(1)}} J_o = (\widehat{A}X)^T \nabla_{\bar{H}^{(2)}} J, \quad \bar{H}^{(2)} = \widehat{A}XW_o^{(1)}. \quad (14)$$

In the flipped space, update $W_f^{(1)}$:

$$\nabla_{W_f^{(1)}} J_f = (\widehat{A}X_f)^T \nabla_{\bar{H}_f^{(2)}} J_f, \quad \bar{H}_f^{(2)} = \widehat{A}X_fW_f^{(1)}. \quad (15)$$

Through the above equations, we can guide the first hyperplane $W^{(1)}$ concurrently.

Proof of convergence. We show that our optimization guarantees the convergence of $W^{(1)}$. If the activation function is origin symmetric, we can redefine Eq. 14 and 15 as below:

$$\begin{aligned} \nabla_{W_o^{(1)}} J_o &= (\widehat{A}X)^T \nabla_{\bar{H}^{(2)}} J_o, \\ \nabla_{W_f^{(1)}} J_f &= -(\widehat{A}(2p_1 - X))^T \nabla_{\bar{H}^{(2)}} J_f. \end{aligned} \quad (16)$$

Here, the gradient of each dimension in $W^{(1)}$ is proportional to X and $X - 2p_1$ in the original and the flipped spaces. Also, it gets closer to a local optimum $W_*^{(1)}$ as the iteration T increases $\mathbb{E}[W_T^{(1)} - W_*^{(1)}]^2 \propto \frac{\log T}{T}$ [Li and Yuan, 2017], and this theorem shows that two-layer neural networks with a ReLU activation converge to a local minimum. Note that gradient ∇J and parameters $|W^{(l)}|, |W_f^{(l)}|$ are all bounded. These properties guarantee the convergence of Flip-GCN [Chen et al., 2017a]. Further, we find that restricting the scale of gradients (α, β) in two spaces can generalize our model:

$$\begin{aligned} W_o &= W_o - \alpha \nabla_{W_o} J_o, \\ W_f &= W_f - \beta \nabla_{W_f} J_f. \end{aligned} \quad (17)$$

3.4 THEORETICAL ANALYSIS

Data augmentation is closely related to empirical risk minimization concerning *bias-variance tradeoff* [Chen et al., 2020b]. Here, we contemplate that flipping, as another augmentation strategy, can generalize the learnable parameters by reducing the variance of predictions. Firstly, let us assume the plane estimator as $g(X_o) = GNN(X_o)$ which is trained only with original feature X_o , and the augmented one as $\bar{g}(X) = GNN(X)$ that uses both features $X = \{X_o \cup X_f\}$. We can easily see that function g is invariant to flipping since $g(X_o, W_o) = g(X_f, W_f)$ since X_f preserves the pair-wise distance between nodes. Since the bias term vanishes under the invariance, we focus on the variance of $g(X)$, which can be decomposed by the law of total variance

$$\begin{aligned} Var(g(X)) &= Var(\mathbb{E}[g(X)]) + \mathbb{E}[Var(g(X))] \\ &= Var(\bar{g}(X)) + \mathbb{E}[Var(g(X))], \end{aligned} \quad (18)$$

where $Var(\mathbb{E}[g(X)]) = Var(\bar{g}(X))$ since they share the same marginal distribution. Here, we exclude the difference of their mean (bias), $\mathcal{W}_1(\mathbb{E}[g(X)], \mathbb{E}[\bar{g}(X)])$, the Wasserstein distance (e.g., L_2) between two distributions and is independent of the total variance. Based on this observation, we can induce the condition below:

$$Var(\bar{g}(X)) \leq Var(g(X)). \quad (19)$$

Finally, we show the losses of two networks follow:

$$\mathcal{L}(\bar{g}(X)) - \mathcal{L}(g(X)) \in -\mathbb{E}[tr(Var(g(X)))] , \quad (20)$$

which means the performance gain of an augmented model depends on the variance of a plane method. Though [Chen et al., 2020b] introduces a tighter bound of Eq. 18 and 20 using *Loewner order*, we omit them here for brevity.

4 EXPERIMENTS

This section describes the experiments for the performance analysis. We focused our efforts to find answers to the following research questions:

Table 2: Node classification accuracy (%) on benchmark datasets. Bold with an asterisk (*) symbol indicates the best performance, and methods with † are built upon GCN. We show α, β that achieves the best accuracy (Eq. 17)

Datasets	Cora	Citeseer	Pubmed	Actor	Chameleon	Squirrel	Cornell	Texas	Wisconsin
Z (Eq. 1)	0.59	0.41	0.96	0.21	1.0	1.0	0.62	0.41	0.53
Homophily (Eq. 21)	0.81	0.74	0.8	0.22	0.23	0.22	0.11	0.06	0.16
MLP	53.2 ± 0.5%	53.7 ± 1.7%	69.7 ± 0.4%	27.9 ± 1.1%	41.2 ± 1.8%	26.5 ± 0.6%	60.1 ± 1.2%	65.8 ± 5.0%	73.5 ± 5.4%
GCN†	79.1 ± 0.7%	67.5 ± 0.3%	77.8 ± 0.2%	20.4 ± 0.6%	49.4 ± 0.7%	31.8 ± 0.9%	39.4 ± 4.3%	47.6 ± 0.7%	40.5 ± 1.9%
DropEdge†	79.0 ± 0.5%	67.4 ± 0.2%	77.0 ± 0.3%	20.2 ± 0.4%	48.9 ± 1.1%	30.9 ± 0.8%	46.7 ± 3.5%	47.5 ± 2.6%	43.3 ± 4.6%
Ortho-GCN†	80.6 ± 0.4%	69.5 ± 0.3%	76.9 ± 0.3%	21.4 ± 1.6%	46.7 ± 0.5%	31.3 ± 0.6%	45.4 ± 4.7%	53.1 ± 3.9%	46.6 ± 5.8%
GIN	77.3 ± 0.8%	66.1 ± 0.6%	77.1 ± 0.7%	24.6 ± 0.8%	49.1 ± 0.7%	28.4 ± 2.2%	42.9 ± 4.6%	53.5 ± 3.0%	38.7 ± 0.5%
GAT	80.1 ± 0.6%	68.0 ± 0.7%	78.0 ± 0.4%	22.5 ± 0.3%	46.9 ± 0.8%	30.8 ± 0.9%	42.1 ± 3.1%	49.2 ± 4.4%	45.8 ± 5.3%
GATv2	79.5 ± 0.5%	67.4 ± 0.6%	76.2 ± 0.5%	22.1 ± 2.0%	48.3 ± 0.4%	28.9 ± 1.2%	38.0 ± 3.8%	52.5 ± 1.7%	41.7 ± 5.1%
APPNP	81.9 ± 0.4%	68.9 ± 0.3%	79.0 ± 0.4%	21.5 ± 0.2%	45.0 ± 0.5%	30.3 ± 0.6%	49.8 ± 3.6%	56.1 ± 0.2%	45.7 ± 1.7%
GCNII	79.6 ± 0.7%	67.0 ± 1.4%	77.8 ± 0.4%	26.1 ± 1.2%	45.1 ± 0.5%	28.1 ± 0.7%	62.5 ± 0.5%	69.3 ± 2.1%	63.2 ± 3.0%
H ₂ GCN	79.5 ± 0.6%	67.4 ± 0.5%	78.7 ± 0.3%	25.8 ± 1.2%	47.3 ± 0.9%	31.1 ± 0.5%	59.8 ± 3.7%	66.3 ± 4.6%	61.5 ± 4.4%
P-reg†	80.0 ± 0.8%	69.2 ± 0.7%	77.4 ± 0.4%	20.9 ± 0.5%	49.1 ± 0.1%	33.6* ± 0.4%	44.9 ± 3.1%	58.5 ± 4.2%	53.7 ± 2.6%
FAGCN	81.0 ± 0.3%	68.3 ± 0.6%	78.9 ± 0.4%	26.7 ± 0.8%	46.8 ± 0.6%	29.9 ± 0.5%	46.5 ± 1.7%	53.8 ± 1.2%	51.0 ± 4.1%
Flip-MLP	61.4 ± 0.7%	60.3 ± 0.5%	74.1 ± 0.5%	35.9* ± 0.5%	43.5 ± 1.2%	28.5 ± 0.8%	70.5* ± 4.1%	79.2* ± 3.6%	80.5* ± 5.1%
vs MLP (+ %)	+ 15.4 %	+ 12.1 %	+ 6.3 %	+ 28.7 %	+ 2.3 %	+ 2.1 %	+ 17.3 %	+ 20.4 %	+ 9.5 %
α, β	1, 0.1	1, 1	1, 0.01	0.1, 0.1	1, 1	1, 1	0.1, 0.1	0.1, 0.01	1, 1
Flip-GCN†	82.7 ± 0.5%	72.4 ± 0.4%	79.2* ± 0.2%	28.6 ± 0.3%	50.4* ± 0.5%	32.4 ± 0.3%	49.4 ± 0.6%	62.2 ± 1.8%	52.3 ± 2.4%
vs GCN (+ %)	+ 4.6 %	+ 7.3 %	+ 1.8 %	+ 40.2 %	+ 2.0 %	+ 1.9 %	+ 20.4 %	+ 30.7 %	+ 29.1 %
α, β	0.1, 0.01	0.01, 0.001	1, 0.01	1e ⁻⁴ , 1e ⁻⁴	1, 1e ⁻⁴	1, 0.01	1, 1e ⁻⁴	1, 1e ⁻⁴	0.01, 0.001
Flip-GAT	83.1* ± 0.6%	72.8* ± 0.4%	78.5 ± 0.2%	30.3 ± 0.8%	48.3 ± 0.3%	31.9 ± 0.5%	51.9 ± 1.4%	61.0 ± 1.1%	54.5 ± 2.1%
vs GAT (+ %)	+ 3.7 %	+ 7.1 %	+ 0.6 %	+ 34.7 %	+ 3.0%	+ 3.6 %	+ 20.2 %	+ 22.0 %	+ 19.0 %
α, β	1, 0.1	0.01, 0.001	1, 0.001	0.1, 0.1	1, 0.1	1, 1	0.1, 1e ⁻⁴	0.1, 1e ⁻⁴	0.1, 0.001

- **RQ1:** Does flipping efficiently solve the problem occurred by multiple zero values in initial features?
- **RQ2:** Does flipping preserve the convergence?
- **RQ3:** How much do the gradients from the original and flipped spaces differ?
- **RQ4:** How does the performance of the flipping method change as the number of training samples vary?

4.1 DATASETS AND BASELINES

Details of datasets. Our experiments are conducted on nine datasets whose statistical details are described in Table 1. We also measure the assortativity of each dataset as below:

$$h = \frac{\sum_{(i,j) \in \mathcal{E}} \mathbb{1}(Y_i = Y_j)}{|\mathcal{E}|}. \quad (21)$$

- **Cora, Citeseer, Pubmed** [Kipf and Welling, 2016] are citation networks, where the node features of Cora and Citeseer are the bag-of-words (binary) while Pubmed consists of TF-IDF values.
- **Actor** [Tang et al., 2009] is an actor co-occurrence graph. The node feature encodes the keywords in the actor’s Wikipedia web pages which only comprises binary values.
- **Chameleon, Squirrel** [Rozemberczki et al., 2019] are from Wikipedia web pages. All features have non-zero positive or negative values. The maximal element of each dataset is 46.4 and 70.4, while the minimum

values are -0.57 and -0.99, which might be inappropriate for our method.

- **Cornell, Texas, Wisconsin**¹ include web pages that are collected from computer science departments of multiple universities. Similar to the citation networks, the node features are bag-of-words (binary).

Baselines. For evaluation, we employ several traditional methods including MLP [Popescu et al., 2009], GCN [Kipf and Welling, 2016], DropEdge [Rong et al., 2019], and GIN [Xu et al., 2018]. Further, we take GAT [Velickovic et al., 2017], GATv2 [Brody et al., 2021], APPNP [Klicpera et al., 2018], GCNII [Chen et al., 2020a], H₂GCN [Zhu et al., 2020], and FAGCN [Bo et al., 2021] for heterophilous graphs. Finally, some algorithms with regularization like P-reg [Yang et al., 2021] and Ortho-GCN [Guo et al., 2022] are used here.

We describe more details of datasets, baselines, and our implementation in Appendix.

4.2 RESULTS AND DISCUSSION (RQ1)

Most importantly, in Table 2, we notice that the three flipping variants (Flip-MLP, Flip-GCN, and Flip-GAT) perform significantly better than their bases (MLP, GCN, and GAT). Now, we analyze these results from two perspectives.

Performance of flipping is sensitive to the value Z. Because flipping is designed to reduce overfitting caused by

¹<http://www.cs.cmu.edu/afs/cs/project/theo-20/www/data/>

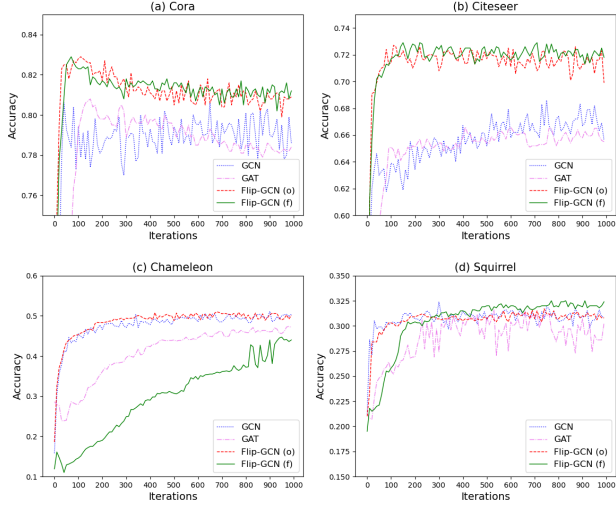


Figure 4: (RQ2) Performance of GCN, GAT, and Flip-GCN as a function of the number of iterations. In Flip-GCN, symbol o and f means original and flipped space, respectively

the sparsity in initial features, we can easily presume that z -value, the non-zero element ratio, is the key factor that determines the performance gains of flipping. Indeed, flipping attains larger performance gains on low z -value datasets than on higher ones. For three datasets with high z -values (Pubmed, Chameleon, and Squirrel), the advancement of flipping over their vanilla models (e.g., Flip-MLP vs MLP) is relatively small. However, all three flipping methods perform better than the original methods achieving average gains of 3 %, 1.9 %, and 2.4 %, respectively, indicating the effectiveness of flipping even for non-zero initials. On another dataset with low z -values, the three flipping variants obtain remarkable advancements over their bases achieving 16.5 %, 24.2 %, and 17.8 % on average. Notably, flipping methods perform best except for Squirrel (with high z and low homophily). This may imply that a slight perturbation to the input features can have a greater impact than aggregation scheme modifications under semi-supervised settings.

The performance is highly related to the homophily ratio. Message passing based GNNs exploit the homophily (Eq. 21) property commonly observed in graphs [Lim et al., 2021, Yan et al., 2021]. Three citation graphs have higher homophily ratios than others. Here, GNNs overwhelm MLP on these homophilic graphs. However, in other datasets like Actor and three WebKB networks, Flip-MLP achieves the best accuracy among the baselines. This implies that message passing fails to generalize well under the high heterophily. Further, the performance gain of Flip-MLP is higher than Flip-GNNs on homophilic graphs, but on heterophilic graphs, GNNs better benefit from the advantages of flipping. Though APPNP performs best on homophilic graphs and some methods (H_2 GCN, FAGCN) outperform GCN on heterophilic networks, our flipping methods surpass

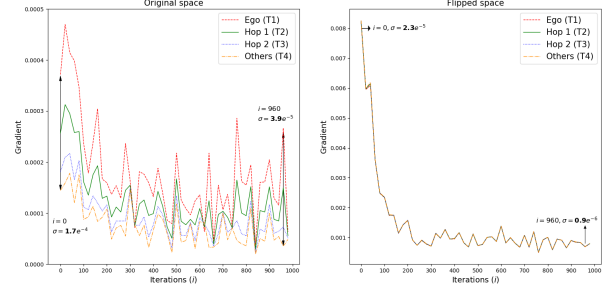


Figure 5: (RQ3) Using the Cora dataset, we plot the magnitude and the standard deviation (σ) of the first projection matrix gradients during training epochs (i)

these algorithms for all graphs.

4.3 CONVERGENCE ANALYSIS (RQ2)

One may argue that flipping may hurt the stability of flipping because it operates on two spaces. Figure 4 plots the performance of two baselines (GCN and GAT) and two flipping methods (Flip-GCN and Flip-GAT) as a function of the number of iterations (one dataset *Texas* is excluded because of a space limitation). The performance of plain GCN (orange), plain GAT (green), flip-GCN (blue), and flip-GAT (red) are plotted with different colors. Here, the x-axis is the training epoch and the y-axis is node classification accuracy.

In Figure 4, we can see that the flipped methods outperform the plain algorithms. Also, compared to the plane GCN and GAT, we notice that flip-based methods experience higher oscillations. We contemplate that this is caused by the gradient updates in the flipped space, where most dimensions are updated at each iteration. Some may argue that the instability of convergence might be risky for neural networks. However, acquiring stable but lower performance with high over-fitting is not the ultimate goal of the problems and we can handle them through the measurement of validation score, which is a widely used strategy for performance evaluation. To summarize, flipping methods achieve better performance than the plain models on datasets with multiple zero elements but we also admit that further investigation has to be conducted for better convergence.

4.4 ANALYSIS OF GRADIENTS ON TWO SPACES (RQ3)

Figure 5 analyzes the gradient of the first projection matrix during the training phase with the Cora dataset. We apply different ranges of neighboring nodes and define four types. The first one (T1) only comprises features of central nodes (Ego). T2 and T3 include features of 1-hop and 2-hop neighbors, respectively. The final (T4) consists of leftover features. We prioritize the types from T1 to T4 to avoid

Table 3: (RQ4) Node classification accuracy (%) w.r.t. the different number of training samples. The symbol (+F) means that flipping is applied on a base method

Dataset	Cora			Chameleon			Cornell			
	L/C	20	40	80	20	40	80	5	10	20
Z	0.59	0.76	0.91	1	1	1	0.62	0.72	0.84	
MLP	53.2	56.9	62.1	41.2	46.3	49.1	60.1	68.8	73.3	
MLP+F	61.4	65.5	70.4	43.5	49.9	51.8	70.5	86.4	95.8	
GCN	79.1	82.8	83.4	49.4	53.5	55.7	39.4	50.7	53.3	
GCN+F	82.7	84.5	85.5	50.4	53.7	55.7	49.4	54.9	72.8	
GAT	80.1	82.4	83.0	46.9	52.4	54.1	42.1	48.9	53.3	
GAT+F	83.1	84.0	84.6	48.3	49.6	53.0	51.9	59.5	64.4	

overlapped features being double-counted. Note that all $T \in \mathcal{R}^F$ are binarized.

In Figure 5, we averaged the magnitude of gradients in two spaces and plot them with different colors. In the original space (left), the features from T1 (red) receive the largest gradient. As described in Eq. 4, the gradients of a neighbor are inversely proportional to its degree. T4 (orange) shows the smallest values suggesting that features are mostly excluded during training (the weight regularization slightly updates the parameters). On the other hand, in flipped space (right), all types tend to have a similar magnitude that conforms to our suggestions; large losses in the flipped space bring large gradients. Thus, we need to adjust them through Eq. 17 during backward propagation.

4.5 VARYING THE SIZE OF TRAINING SAMPLES (RQ4)

As we pointed out before, the root cause that deteriorates the performance of semi-supervised learning is the lack of labeled samples. Thus, we scrutinize the effect of labeled sample size on performance by adjusting the scale of training samples. In Table 3, we show the z-value of central nodes based on the number of labeled nodes per class (L/C). Due to the space limitation, we exclude *Wisconsin* here.

From the above result, GCN and GAT outperform MLP since the above two datasets are quite assortative (please see Homophily in Table 2). At the same time, we can observe that the performance gain of flipping decreases as the L/C increases. The reason is that as more training nodes are available, the initial features start to cover most dimensions (large z-value) such that plain models can update the first weight matrix. However, for some datasets (Chameleon, Squirrel) whose entire features are non-zero, we notice that flip merely affect the overall quality as the number of samples increase. Remember that all elements of the initial features of these datasets are non-zero (Z is 1) and their maximal values are high. Thus, as the labeled node increases, the vanilla GCN shows good performance since a first hyperplane might generalize well without flipping. This also happens to GAT, where the performance gap between GAT and GAT+F becomes smaller as L/C rises. In WebKB graphs (Cornell,

Texas, Wisconsin), the accuracy of all methods grows almost exponentially w.r.t. the L/C samples. Throughout these results, we contemplate that integrating a flipping can secure robustness and generalize to certain kinds of features.

5 RELATED WORK

Graph Neural Networks. Generally, most GNNs can be classified into two types; spectral-based and spatial-based algorithms. The first one established a mathematical foundation of conducting graph convolution operation in a spectral domain using the Laplacian matrix [Bruna et al., 2013, Defferrard et al., 2016, Dong et al., 2021]. Spatial-based GNNs aggregate the information of local neighborhoods from spatial perspectives, and ignited many aggregation scheme developments for the handling of noisy connections [Velickovic et al., 2017, Pei et al., 2020, Zhu et al., 2020, Chien et al., 2020, Bo et al., 2021]. Compared to the noisy neighbor problem, the problem incurred by the sparse initial features has not received much research attention.

Generalization of neural networks. Many approaches have been proposed for the generalization of parameters in neural networks [Chen et al., 2017a, Feng and Simon, 2017, Wang et al., 2021]. Several suggested the normalization of deep neural networks [Huang et al., 2020] while others applied regularization to all adjacent nodes [Yang et al., 2021] or integrated label propagation to give further information [Wang and Leskovec, 2020]. More recently, the orthogonal GCN [Guo et al., 2022] attacks the gradient vanishing problem at the initial few layers of GNNs. RawlsGCN [Kang et al., 2022] claims the unfairness of gradient update which is biased to nodes with a large degree. Though these methods show notable improvements under the semi-supervised scenario, they fail to solve the problem that is inherently occurred by a characteristic of initial features. In this paper, we aim to solve this limitation through the generalization of the first hyperplane.

6 CONCLUSION

Existing GNNs mainly focus on the tuning of aggregation strategy, while the type of initial features is unconsidered. In this work, we investigate the theoretical relationship between the zero elements of input vectors and their impact on the first layer of neural networks. We then propose a co-training in both the original and flipped spaces, which learns the gradient flows from both channels and adaptively adjusts the parameters. We provide an analysis of the backpropagation and empirical studies on nine real-world benchmark datasets. Equipping three base methods with flipping improves the node classification accuracy, which indicates that our suggestion is highly scalable and competitive. In future work, we expect the application of flipping with many other

variations of GNNs to enhance their quality.

REFERENCES

- [Bo et al., 2021] Bo, D., Wang, X., Shi, C., and Shen, H. (2021). Beyond low-frequency information in graph convolutional networks. *arXiv preprint arXiv:2101.00797*.
- [Brody et al., 2021] Brody, S., Alon, U., and Yahav, E. (2021). How attentive are graph attention networks? *arXiv preprint arXiv:2105.14491*.
- [Bruna et al., 2013] Bruna, J., Zaremba, W., Szlam, A., and LeCun, Y. (2013). Spectral networks and locally connected networks on graphs. *arXiv preprint arXiv:1312.6203*.
- [Cai et al., 2021] Cai, T., Luo, S., Xu, K., He, D., Liu, T.-y., and Wang, L. (2021). Graphnorm: A principled approach to accelerating graph neural network training. In *International Conference on Machine Learning*, pages 1204–1215. PMLR.
- [Chen et al., 2017a] Chen, J., Zhu, J., and Song, L. (2017a). Stochastic training of graph convolutional networks with variance reduction. *arXiv preprint arXiv:1710.10568*.
- [Chen et al., 2020a] Chen, M., Wei, Z., Huang, Z., Ding, B., and Li, Y. (2020a). Simple and deep graph convolutional networks. In *International Conference on Machine Learning*, pages 1725–1735. PMLR.
- [Chen et al., 2020b] Chen, S., Dobriban, E., and Lee, J. H. (2020b). A group-theoretic framework for data augmentation. *The Journal of Machine Learning Research*, 21(1):9885–9955.
- [Chen et al., 2017b] Chen, Y., Li, J., Xiao, H., Jin, X., Yan, S., and Feng, J. (2017b). Dual path networks. *Advances in neural information processing systems*, 30.
- [Chien et al., 2020] Chien, E., Peng, J., Li, P., and Milenkovic, O. (2020). Adaptive universal generalized pagerank graph neural network. *arXiv preprint arXiv:2006.07988*.
- [Defferrard et al., 2016] Defferrard, M., Bresson, X., and Vandergheynst, P. (2016). Convolutional neural networks on graphs with fast localized spectral filtering. *Advances in neural information processing systems*, 29.
- [Dong et al., 2021] Dong, Y., Ding, K., Jalaian, B., Ji, S., and Li, J. (2021). Graph neural networks with adaptive frequency response filter. *arXiv preprint arXiv:2104.12840*.
- [Feng and Simon, 2017] Feng, J. and Simon, N. (2017). Sparse-input neural networks for high-dimensional non-parametric regression and classification. *arXiv preprint arXiv:1711.07592*.
- [Gilmer et al., 2017] Gilmer, J., Schoenholz, S. S., Riley, P. F., Vinyals, O., and Dahl, G. E. (2017). Neural message passing for quantum chemistry. In *International conference on machine learning*, pages 1263–1272. PMLR.
- [Guo et al., 2022] Guo, K., Zhou, K., Hu, X., Li, Y., Chang, Y., and Wang, X. (2022). Orthogonal graph neural networks. In *Proceedings of the AAAI Conference on Artificial Intelligence*, volume 36, pages 3996–4004.
- [Hamilton et al., 2017] Hamilton, W., Ying, Z., and Leskovec, J. (2017). Inductive representation learning on large graphs. *Advances in neural information processing systems*, 30.
- [Huang et al., 2020] Huang, L., Qin, J., Zhou, Y., Zhu, F., Liu, L., and Shao, L. (2020). Normalization techniques in training dnns: Methodology, analysis and application. *arXiv preprint arXiv:2009.12836*.
- [Jin et al., 2021] Jin, W., Derr, T., Wang, Y., Ma, Y., Liu, Z., and Tang, J. (2021). Node similarity preserving graph convolutional networks. In *Proceedings of the 14th ACM international conference on web search and data mining*, pages 148–156.
- [Kang et al., 2022] Kang, J., Zhu, Y., Xia, Y., Luo, J., and Tong, H. (2022). Rawlsgcn: Towards rawlsian difference principle on graph convolutional network. In *Proceedings of the ACM Web Conference 2022*, pages 1214–1225.
- [Kim and Oh, 2022] Kim, D. and Oh, A. (2022). How to find your friendly neighborhood: Graph attention design with self-supervision. *arXiv preprint arXiv:2204.04879*.
- [Kim et al., 2019] Kim, H., Rasch, M., Gokmen, T., Ando, T., Miyazoe, H., Kim, J.-J., Rozen, J., and Kim, S. (2019). Zero-shifting technique for deep neural network training on resistive cross-point arrays. *arXiv preprint arXiv:1907.10228*.
- [Kipf and Welling, 2016] Kipf, T. N. and Welling, M. (2016). Semi-supervised classification with graph convolutional networks. *arXiv preprint arXiv:1609.02907*.
- [Klicpera et al., 2018] Klicpera, J., Bojchevski, A., and Günnemann, S. (2018). Predict then propagate: Graph neural networks meet personalized pagerank. *arXiv preprint arXiv:1810.05997*.
- [Li and Yuan, 2017] Li, Y. and Yuan, Y. (2017). Convergence analysis of two-layer neural networks with relu activation. *Advances in neural information processing systems*, 30.
- [Lim et al., 2021] Lim, D., Hohne, F., Li, X., Huang, S. L., Gupta, V., Bhalerao, O., and Lim, S. N. (2021). Large scale learning on non-homophilous graphs: New benchmarks and strong simple methods. *Advances in Neural Information Processing Systems*, 34:20887–20902.

- [Lin et al., 2020] Lin, M., Ji, R., Xu, Z., Zhang, B., Wang, Y., Wu, Y., Huang, F., and Lin, C.-W. (2020). Rotated binary neural network. *Advances in neural information processing systems*, 33:7474–7485.
- [Liu et al., 2022] Liu, H., Hu, B., Wang, X., Shi, C., Zhang, Z., and Zhou, J. (2022). Confidence may cheat: Self-training on graph neural networks under distribution shift. In *Proceedings of the ACM Web Conference 2022*, pages 1248–1258.
- [Luo et al., 2021] Luo, D., Cheng, W., Yu, W., Zong, B., Ni, J., Chen, H., and Zhang, X. (2021). Learning to drop: Robust graph neural network via topological denoising. In *Proceedings of the 14th ACM International Conference on Web Search and Data Mining*, pages 779–787.
- [McPherson et al., 2001] McPherson, M., Smith-Lovin, L., and Cook, J. M. (2001). Birds of a feather: Homophily in social networks. *Annual review of sociology*, 27(1):415–444.
- [Pei et al., 2020] Pei, H., Wei, B., Chang, K. C.-C., Lei, Y., and Yang, B. (2020). Geom-gcn: Geometric graph convolutional networks. *arXiv preprint arXiv:2002.05287*.
- [Popescu et al., 2009] Popescu, M.-C., Balas, V. E., Perescu-Popescu, L., and Mastorakis, N. (2009). Multi-layer perceptron and neural networks. *WSEAS Transactions on Circuits and Systems*, 8(7):579–588.
- [Rong et al., 2019] Rong, Y., Huang, W., Xu, T., and Huang, J. (2019). Dropedge: Towards deep graph convolutional networks on node classification. *arXiv preprint arXiv:1907.10903*.
- [Rozemberczki et al., 2019] Rozemberczki, B., Davies, R., Sarkar, R., and Sutton, C. (2019). Gemsec: Graph embedding with self clustering. In *Proceedings of the 2019 IEEE/ACM international conference on advances in social networks analysis and mining*, pages 65–72.
- [Shijie et al., 2017] Shijie, J., Ping, W., Peiyi, J., and Siping, H. (2017). Research on data augmentation for image classification based on convolution neural networks. In *2017 Chinese automation congress (CAC)*, pages 4165–4170. IEEE.
- [Singla et al., 2021] Singla, V., Ge, S., Ronen, B., and Jacobs, D. (2021). Shift invariance can reduce adversarial robustness. *Advances in Neural Information Processing Systems*, 34:1858–1871.
- [Tang et al., 2009] Tang, J., Sun, J., Wang, C., and Yang, Z. (2009). Social influence analysis in large-scale networks. In *Proceedings of the 15th ACM SIGKDD international conference on Knowledge discovery and data mining*, pages 807–816.
- [Velickovic et al., 2017] Velickovic, P., Cucurull, G., Casanova, A., Romero, A., Lio, P., and Bengio, Y. (2017). Graph attention networks. *stat*, 1050:20.
- [Wang and Leskovec, 2020] Wang, H. and Leskovec, J. (2020). Unifying graph convolutional neural networks and label propagation. *arXiv preprint arXiv:2002.06755*.
- [Wang et al., 2021] Wang, X., Liu, H., Shi, C., and Yang, C. (2021). Be confident! towards trustworthy graph neural networks via confidence calibration. *Advances in Neural Information Processing Systems*, 34:23768–23779.
- [Xiao et al., 2021] Xiao, T., Chen, Z., Wang, D., and Wang, S. (2021). Learning how to propagate messages in graph neural networks. In *Proceedings of the 27th ACM SIGKDD Conference on Knowledge Discovery & Data Mining*, pages 1894–1903.
- [Xu et al., 2018] Xu, K., Hu, W., Leskovec, J., and Jegelka, S. (2018). How powerful are graph neural networks? *arXiv preprint arXiv:1810.00826*.
- [Yan et al., 2021] Yan, Y., Hashemi, M., Swersky, K., Yang, Y., and Koutra, D. (2021). Two sides of the same coin: Heterophily and oversmoothing in graph convolutional neural networks. *arXiv preprint arXiv:2102.06462*.
- [Yang et al., 2021] Yang, H., Ma, K., and Cheng, J. (2021). Rethinking graph regularization for graph neural networks. In *Proceedings of the AAAI Conference on Artificial Intelligence*, volume 35, pages 4573–4581.
- [Yang et al., 2019] Yang, L., Wu, F., Wang, Y., Gu, J., and Guo, Y. (2019). Masked graph convolutional network. In *IJCAI*, pages 4070–4077.
- [Ying et al., 2019] Ying, Z., Bourgeois, D., You, J., Zitnik, M., and Leskovec, J. (2019). Gnnexplainer: Generating explanations for graph neural networks. *Advances in neural information processing systems*, 32.
- [Zhang et al., 2017] Zhang, X., Liu, L., Xie, Y., Chen, J., Wu, L., and Pietikainen, M. (2017). Rotation invariant local binary convolution neural networks. In *Proceedings of the IEEE International Conference on Computer Vision Workshops*, pages 1210–1219.
- [Zhu et al., 2020] Zhu, J., Yan, Y., Zhao, L., Heimann, M., Akoglu, L., and Koutra, D. (2020). Beyond homophily in graph neural networks: Current limitations and effective designs. *Advances in Neural Information Processing Systems*, 33:7793–7804.
- [Zhu et al., 2021] Zhu, Y., Xu, Y., Yu, F., Liu, Q., Wu, S., and Wang, L. (2021). Graph contrastive learning with adaptive augmentation. In *Proceedings of the Web Conference 2021*, pages 2069–2080.